Online Gait Transitions and Disturbance Recovery for Legged Robots via the Feasible Impulse Set

Article · January 2019

DOI: 10.1109/LRA.2019.2896723

6 authors, including:

Chiheb Boussema
Carnegie Mellon University
4 PUBLICATIONS **3** CITATIONS
SEE PROFILE

Gerardo Bledt
Massachusetts Institute of Technology
12 PUBLICATIONS **68** CITATIONS
SEE PROFILE

A.J. Ijspeert
École Polytechnique Fédérale de Lausanne
417 PUBLICATIONS **13,699** CITATIONS
SEE PROFILE

Patrick Wensing
University of Notre Dame
42 PUBLICATIONS **489** CITATIONS
SEE PROFILE

Author Pre-Print Copy. Please see official version at:
http://dx.doi.org/10.1109/LRA.2019.2896723

Online Gait Transitions and Disturbance Recovery for Legged Robots via the Feasible Impulse Set

Chiheb Boussema[1,2], Matthew J. Powell[1], Gerardo Bledt[1], Auke J. Ijspeert[2], Patrick M. Wensing[3] and Sangbae Kim[1]

***Abstract*—Gaits in legged robots are often hand-tuned and time-based, either explicitly or through an internal clock, for instance in the form of central pattern generators. This strategy requires trial and error to identify leg timings, which may not be suitable in challenging terrains. In this paper, we introduce new concepts to quantify leg capabilities for online gait emergence and adaptation, without fixed timings or predefined foothold sequences. Specifically, we introduce the Feasible Impulse Set, a notion that extends aspects of the classical wrench cone to include a prediction horizon into the future. By considering the impulses that can be delivered by the legs, quantified notions of leg utility are proposed for coordinating adaptive lift-off and touch-down of stance legs. The proposed methods provide push recovery and emergent gait transitions with speed. These advances are validated in experiments with the MIT Cheetah 3 robot, where the framework is shown to automatically coordinate aperiodic behaviors on a partially-moving walkway.**

***Index Terms*—Legged Robots, Motion Control, Underactuated Robots.**

I. Introduction

ANIMAL locomotion has long been under investigation with the desire to replicate biological gaits in mechanical automata. However, even within biology, no consensus has been reached regarding the precise determinants of gait [1]. Hypotheses considering energetic optimality are most common [2], [3]. Alternate studies considering, e.g., mechanical comfort suggest other factors also play a role [4], [5]. This lack of consensus, in part, challenges the application of bio-inspired approaches for gait generation in robot systems.

To date, several approaches have been proposed for gait selection and design in legged robots. One route is to optimize gaits with respect to energy consumption, mechanical strain, or other heuristically-designed combinations of factors.

[1]Chiheb Boussema, Matthew J. Powell, Gerardo Bledt and Sangbae Kim are with the Department of Mechanical Engineering, Massachusetts Institute of Technology, Cambridge, MA, 02139 USA sangbae@mit.edu

[2]Chiheb Boussema and Auke J. Ijspeert are with the Institute of Bioengineering, Ecole Polytechnique Fédérale de Lausanne, CH-1015 Switzerland chiheb.boussema@alumni.epfl.ch | auke.ijspeert@epfl.ch

[3]Patrick M. Wensing is with the Department of Aerospace and Mechanical Engineering, University of Notre Dame, IN, 46556 USA pwensing@nd.edu

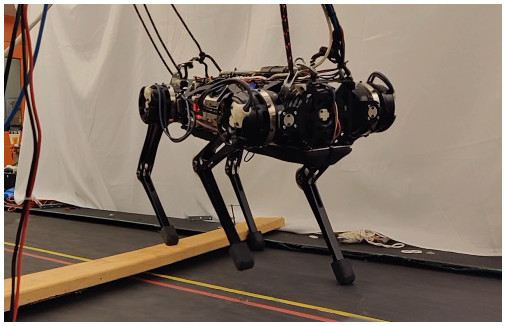

Fig. 1. Aperiodic locomotion on a partially-moving surface. Gait sequences automatically adapt to this unmodeled environmental context.

Wampler and Popović [6] used a combination of gradient-based spacetime optimization and derivative-free methods to optimize for gait sequences, motions, and morphology. In [7], the authors used particle swarm optimization over forward velocity, concluding that environmental constraints were an important factor in gait adoption. These studies provide useful offline tools for generating gaits or studying hypotheses relating to biological systems. However, other approaches are required for online application with robots in diverse terrains.

To enable operation in challenging terrains, others have borrowed inspiration from biological central pattern generators (CPGs). CPGs have been used for the control of quadrupedal and sprawled-posture robots within a nonlinear dynamical systems framework (see, e.g., [1], [8], [9]). Many studies explicitly design CPGs to produce specific gaits, without providing insights or principles for gait selection [1].

In contrast, a subset of the CPG literature (e.g., [10]–[13]) has proposed the use of sensory feedback to modulate weakly-coupled oscillators. Feedback from leg loading and/or body tilting couples the dynamics of the robot and the environment, leading to environmentally- and morphologically-driven emergent gait transitions. Nonetheless, due to their reliance on an oscillating internal clock, generative procedures for designing stabilizing feedback remain unclear and limited to periodic movement.

In parallel, model-based control approaches within the community have provided an alternate avenue to online gait generation and adaptation. Impedance-based control strategies in the MIT Cheetah 1 [14] and impulse-based control in the MIT Cheetah 2 [15] have demonstrated high-speed trotting, bounding, and galloping over various surfaces. Model-predictive control (MPC) has been a main strategy to

generalize these results to a variety of gaits [16]–[18] and for jumping over obstacles [19]. While the above-mentioned works used adjustable predefined foot trajectories, [20] used an MPC framework to optimize foot placements following a prescribed foot timing and sequencing. By contrast, phase-based parametrization of optimization variables in [21] allowed the use of nonlinear programming to automatically plan timing and footholds for highly dynamic motions. Mixed-integer techniques also enabled planning gait sequences for both locomotion [22] and multi-contact balancing [23] at the expense of potential combinatorial increases in complexity.

Toward reducing computational complexity for online optimization, much work has concentrated on selecting contact sequences through consideration of the contact wrench cone (CWC). The CWC describes the net forces and moments that can be delivered to the robot given a set of friction-limited contacts. Work centered on the CWC has provided efficient algorithms leveraging polyhedral convex geometry to compute regions of static equilibrium [24], to address robustness for these regions [25], [26], or to plan CoM motions with dynamic constraints [27], [28]. Recent work [29] addressed actuator limitations for wrench cones, improving translation of the method to hardware. Despite these reductions, formulations with the flexibility to choose gait sequences remain computationally prohibitive for online use.

At a high level, it is noted that time and movement are inherently inseparable. This observation suggests diverting our attention from forces to impulses[1] (i.e., forces over time) when it comes to selecting the timing and locations of contacts. Toward this end, the contribution of this paper is a new framework for generating adaptive gaits by considering the set of impulses that can be generated by the contact legs, individually and combined. We name such a set a Feasible Impulse Set (FIS), and propose a new set of tools for emergent gait generation based upon the concept.

To enable online gait adaptation, the methods consider new simple and physically-intuitive metrics of leg utility. In brief, they measure the remaining impulse capabilities in stance, and the relative importance of these limb-specific capabilities with respect to the other supporting limbs. Adaptive foot touchdown and liftoff conditions based on these metrics are shown to enable variable-speed locomotion with emergent gait sequences and aperiodic behaviors in response to disturbances or challenging environmental contexts (e.g., as in Fig. 1). Extensive tests on the MIT Cheetah 3 robot show promise for this new gait control framework. While we here discuss quadruped locomotion, the framework provided is able to accommodate general multilegged robots.

Paper organization: This paper is organized as follows. Section II-A and II-B present the central notions of feasible force and impulse sets. Section II-C presents the leg utility metrics required for the introduction of the leg utility control method presented in Section III. In Section IV we present results from hardware and simulation experiments on the MIT Cheetah 3, followed by a broad discussion in Section V.

[1]This does not imply impulsive locomotion as in jumps but rather the integration of force over time.

II. Leg Utility Control Framework

A. Feasible Force Set

Assuming minimal inertial effects, foot forces and joint torques are related through a Jacobian mapping $\tau = J^T F$, where J is the leg Jacobian. Only a limited set of ground reaction forces can be generated based on the torque limits of actuators in each leg:

$$\underline{\tau} \leq J^T F \leq \bar{\tau} \tag{1}$$

where $\underline{\tau}$ and $\bar{\tau}$ are the torque limits of the motors. Forces must also respect friction limits to avoid slipping. Assuming Coulomb friction, the friction cone is often linearized as

$$AF \leq 0 \tag{2}$$

where the matrix A is as given in [30]. Combining (1) and (2), we obtain the following inequality, for the 2D case:

$$PF \leq b \tag{3}$$

where

$$P = \begin{bmatrix} A^T & J & -J \end{bmatrix}^T;\ F = \begin{bmatrix} F_x & F_z \end{bmatrix}^T;\ b = \begin{bmatrix} 0 & \bar{\tau}^T & -\underline{\tau}^T \end{bmatrix}^T.$$

The inequality (3) is used to define a Feasible Force Set (FFS), $\mathscr{F}$ as:

$$\mathscr{F} = \{F \mid PF \leq b\} \tag{4}$$

Note that since the leg Jacobian J depends on configuration, so too does $\mathscr{F}$. This definition is valid for either a 2D or 3D FFS (where the dimensions of the variables have to be adjusted). The set $\mathscr{F}$ is a convex set, and more specifically is a convex polytope. FFSs appear in other applications, e.g., in [30] for force distribution within post-impact control of fall recovery and in [29] for trajectory optimization.

B. Feasible Impulse Set

1) Preliminaries: The following assumes familiarity with a few concepts from polyhedral computational geometry that are briefly reviewed. A convex polytope (CP) is a convex set that can be described as the convex hull of a finite set of points. Such a set can be represented in one of two compact forms: though a set of inequalities that define its faces (i.e., as in (4)), or through the specification of its extremal points (i.e., its vertices). Conversion between these representations can be accomplished using linear programming [31]. Given two CPs X and Y, the sum of these sets $X \bigoplus Y = \{x+y \mid x \in X,\ y \in Y\}$ is called their Minkowski sum. This set can also be viewed as the convex hull of the set of points that results by adding *every* vertex of one convex polytope to *every* vertex of the other. The reader is referred to [30] Sec. II-B for further introduction, and to [31] for more detail.

2) Feasible Impulse Set: We assess the value of each supporting limb based on the impulses that it can generate. This calculation of leg utility is based on a feasible impulse set (FIS) that arises from considering the sum of FFSs over a nominal trajectory in time. Thus, a FIS can be viewed as a discrete integral of sets of feasible forces. More precisely, we construct the FIS by Minkowski-summing the instantaneous FFSs multiplied by an appropriate time increment δt, over

a time window ΔT, or equivalently from an initial to a final configuration. Mathematically, the FIS, $\hat{\mathscr{F}}$, is given by[2]

$$\hat{\mathscr{F}} = \bigoplus \mathscr{F}_i \cdot \delta t_i, \tag{5}$$

where $\mathscr{F}_i$ is the FFS at a particular leg configuration (i.e., a foot position relative to the hip), and i spans ΔT such that $\sum_i \delta t_i = \Delta T$ over configurations sweeping from an initial foot position, x_{init}, to a final one, x_f. Here, constant height is assumed and the foot position x_i is a scalar. The LRS library [32] is used to convert the FFSs (given by (4)) to their vertex representation before applying the Minkowski sum. The computations assume a constant body velocity over each δt_i, which allows the prediction of the foot trajectory.

A FIS computed from an initial foot position x_0 to a final position x_f may be referred to as $\hat{\mathscr{F}}_{x_0 \to x_f}$, with a special case $\hat{\mathscr{F}}_{x_0 \to lim}$ meaning that x_f is the limit of the workspace. In what follows, $\hat{\mathscr{F}}$ will be used to refer to $\hat{\mathscr{F}}_{x_0 \to lim}$, unless otherwise mentioned. Note that since the Minkowski sum of two convex polytopes (CPs) is a CP, then the FIS is also a CP, thus keeping the associated computational benefits.
Here we present some notes to take into consideration when computing the FIS:

1) Eq. (5) holds for 2D and 3D. However, 3D computations present scalability challenges that may become too heavy for online use. Further discussion of 3D extension is given in Sec. V.
2) To ease calculations and for ease of use, we (a) take $\delta t_i = \delta t = \Delta T/(N-1)$, where N is the number of configurations i at which the FFSs were computed, and (b) assume a constant speed during the time span ΔT.
3) The FFS varies smoothly with leg configuration, and the possible leg configurations swept by the stance leg are limited.

Let us further introduce the following definition:

Definition 1. ***Nodes****, $x_1, \cdots, x_N$, are foot positions relative to the corresponding hip, where a positive x is in the forward direction of travel.*

Considering points (2)-(3) above and Def. 1, the FFS and an associated precursor to the FIS can be pre-computed offline for each node. The latter, which we shall denote pFIS, or $p\hat{\mathscr{F}}$, is computed as $p\hat{\mathscr{F}}_i = \bigoplus \mathscr{F}_k \ ; \ k = i, \cdots, n$ (where n is such that $x_n = x_f$). A factor δt can then be applied online to compute the FIS based on speed[3]. With this factor, the pFIS is related to the FIS in a simple manner $\hat{\mathscr{F}} = p\hat{\mathscr{F}} \cdot \delta t$ when assuming a constant average speed over equally-spaced nodes. With this assumption, we shall concentrate development on the FIS in the remainder of this letter, while heavy use is made of the pFIS for a computationally-efficient implementation.

C. Leg Utility

For the robot (or a living being for that matter) to be able to perform any maneuver, including walking, it needs to have a sense of its physical abilities. We conjecture that a sense of impulse generation capabilities is of primary importance for locomotion. One can use the volume of the FIS as a metric in this regard; the larger the volume, the greater the capabilities. Other measures of impulse capability can also be considered. For instance, the radius of the Chebyshev sphere centered at $\hat{F}$ is a measure that gives a sense of safety relative to a desired impulse $\hat{F}$. This metric has been used in, e.g., [28], [33] with the CWC. In what follows we choose to use the volume of the FIS as a capacity measure, since it is readily available upon computation of the set. Note that for 2D polytopes, we make an abuse of language and refer to the area of the convex hull as volume.

1) Marginal Utility: For a multi-legged robot, we define the marginal utility, U^*, of leg l as

$$U_l^* = 1 - V_{\oplus_{j \neq l}} \Big/ V_{all} \tag{6}$$

where $V_{\oplus_{j \neq l}}$ is the volume of the Minkowski sum of the FIS of all contact legs, except leg l, and V_{all} is the volume of the Minkowski sum of the FIS for all contact legs. The value of U^* thus depends on the configuration of all contact legs. This metric gives information on how much one loses in terms of impulse generation by not having leg l on the ground. The higher the value, the more useful the leg is. The marginal utility metric gives a sense of the cooperation that should take place between legs in supporting the body.

2) Utility: Given a foot position x_i for leg l, the leg's utility U_l is defined as

$$U_l = V(\hat{\mathscr{F}}_{x_i \to lim}) \Big/ V(\hat{\mathscr{F}}_{x_0 \to lim}) \tag{7}$$

where x_0 is the foot position at touchdown and $V(\cdot)$ is the volume of the set. This metric quantifies the usefulness of a leg in terms of remaining impulse generation capabilities.

3) Agility Metrics: For previous metrics, though we quantify leg capabilities in the direction of travel, the information does not provide a complete picture of what a leg can do. To get a sense of the agility of a leg (i.e., its ability to provide different types of impulses), we introduce the following.

Definition 2. ***Forward movement FIS****, $\hat{\mathscr{F}}^\sharp$, denotes a $\hat{\mathscr{F}}$ along nodes $x_1, \cdots, x_N$ that correspond to a forward motion of the body relative to a stance foot, i.e., $x_1 > \cdots > x_N$.*

Definition 3. ***Backward movement FIS****: $\hat{\mathscr{F}}^\flat$ denotes a $\hat{\mathscr{F}}$ along nodes $x_1, \cdots, x_N$ that correspond to a backward motion of the body relative to a stance foot, i.e., $x_1 < \cdots < x_N$.*

We further introduce the following sign convention. A positive force is one that pushes the robot in the forward direction of motion. A negative force does the opposite. With this, we denote the positive FIS, $\hat{\mathscr{F}}^\oplus$ as the subset of positive impulses within $\hat{\mathscr{F}}$, and the negative FIS, $\hat{\mathscr{F}}^\ominus$, as the subset of negative impulses within $\hat{\mathscr{F}}$. The notations are naturally expanded to the forward and backward movement FISs to have a combination of positive/negative forward/backward movement FIS: $\hat{\mathscr{F}}^{\sharp\oplus}$, $\hat{\mathscr{F}}^{\flat\oplus}$, $\hat{\mathscr{F}}^{\sharp\ominus}$, and $\hat{\mathscr{F}}^{\flat\ominus}$.

We emphasize that the sharp and flat notation $\sharp, \flat$ corresponds to body movements in space, whereas the plus and

[2]Note that by the notation $\mathscr{X} \cdot \delta t$ we mean that the scaling factor δt applies to the vertices of $\mathscr{X}$, i.e., if $\tilde{\mathscr{X}} = \mathscr{X} \cdot \delta t$, then $\tilde{\mathscr{X}} = \{\delta t \ x \mid x \in \mathscr{X}\}$.

[3]We used a $\delta t = \delta / \bar{v}$, where $\bar{v}$ is average speed and δ is the internode distance, as per Def. 1

minus notation $\oplus$, $\ominus$ refers to directions (fore/aft) of impulses. For example, $\hat{\mathscr{F}}^{\flat\oplus}$ is the set of positive impulses (generating forward velocity) that could be generated by a backward-moving robot.

III. Locomotion Control Strategy

Based on the above framework consisting of the various FISs and the leg utility metrics, we designed a locomotion control strategy capable of autonomous gait emergence and adaptation to and recovery from disturbances like pushes.

A. Touchdown foot placement

Several strategies can be employed to select a touch-down position. One option could be to compute different variations of the FIS ($\hat{\mathscr{F}}^{\sharp\oplus}$, $\hat{\mathscr{F}}^{\sharp\ominus}$, $\hat{\mathscr{F}}^{\flat\oplus}$, and $\hat{\mathscr{F}}^{\flat\ominus}$), then find the position that achieves a desired trade-off between the volumes of these FISs. For example, one may be more wary of disturbances that would make the robot tumble forward (versus disturbances that would push it backward), and therefore may want to step such that the volume of $\hat{\mathscr{F}}^{\sharp\ominus}$ that is significantly higher than that of $\hat{\mathscr{F}}^{\flat\oplus}$. This means that the foot location would provide stronger abilities to stop a forward push than a backward one.

Another option would be to choose a position that has a sufficiently good deceleration impulse ability and not just propelling power. This may also depend on the leg and its intended function (e.g., weight bearing vs. propulsion). The general workflow for choosing a touchdown foot position is summarized in Fig. 2. The figure also shows two tradeoff ratios (blue and orange), each making use of two FIS variants, as a function of foot position (as explained in the figure caption.) Practically, we use the ratio of braking versus propulsive capability shown in blue in Fig. 2 as a trade-off for forward motion, and a similar one, using the backward FISs, for backward motion. Trade-off ratios are computed offline, but the choice of which ratio to use is done online, allowing seamless transitions between directions of motion.

In addition to these strategies, one can choose the foot position such that a desired impulse $\hat{F}_d \in \hat{\mathscr{F}}$ (which we do for push recovery in a paragraph below). One may further add a condition on the distance of $\hat{F}_d$ to the closest edge (or face) of $\hat{\mathscr{F}}$. As mentioned above and in Sec. IV, we only use 2 simple ratios of 2 FIS volumes at a time (depending on the direction of motion). However, many other trade-off or weighting strategies could be employed and changed online depending on the situation. Note that all these strategies can as well be used for any other direction of motion by replacing forward and backward by the appropriate direction.

B. Swing command

For the swing command we followed the simple rule that is the basis for this work: if the utility of a leg falls below a threshold then this leg should be "recycled" by a swing command. This condition alone, however, is not sufficient to allow for stable locomotion and meaningful interlimb coordination. We thus designed a multi-layered swing control algorithm as follows:

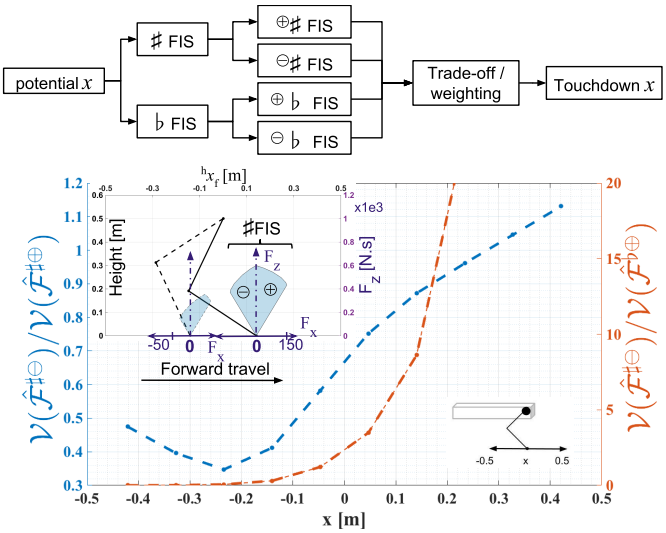

Fig. 2. (Top) General workflow for foot placement at touchdown. (Bottom) Two tradeoff ratios for foot placement at touchdown: (left) emphasize decelerating impulse capability relative to propelling impulse capability, and (right) emphasize the ability to stop a forward push relative to the ability to stop a backward push. Top left inset: 2 leg configurations with associated forward FIS and their $\oplus$ and $\ominus$ subsets ($\delta t = 0.1s$ for illustrative purposes).

1) *Leg utility control*: if $U < \bar{U}$ then the leg is initially allowed to enter swing phase ($\bar{U}$ is a threshold).
2) *Leg marginal utility control*: If $U^\star < \bar{U}^\star$ then the leg is allowed to enter swing phase.
3) *Neighboring legs check*: If any neighboring legs[4] are in swing then the leg in question remains in stance.[5]
4) *Remaining workspace check*: If the foot is close to its workspace limit, then the neighboring legs are commanded to stop their swing phase and plant, allowing the current leg to enter swing phase.

C. Push Recovery

A generalization of the above touchdown decision making algorithm allows for push recovery that is inherently applicable to multi-legged robots and automatically extendable to N-step recovery via repeated single-step re-planning. The key is to place the foot at a location such that the recovery impulse $\hat{F}_{rec} \in \hat{\mathscr{F}}$, where $\hat{\mathscr{F}}$ is the combined FIS of all stance legs. In practice, the FIS for push recovery is computed online, benefiting from the offline computations of the FFSs at the predefined nodes (see caption of Fig. 3). Swing onset can be kept as above (which we do) or adjusted according to insights from the FIS. The flowchart in Fig. 3 summarizes the push recovery algorithm by an example.

IV. Results

The control strategy presented in Section III was applied to the quadruped MIT Cheetah 3 [34] in a 3D dynamic simulation and on the experimental robot fully unconstrained

[4]For the front right leg of a quadruped for instance, the neighboring legs are the front left and the hind right.

[5]This rule will eventually be replaced by a more general one motivated by an 'angular momentum impulse set' to allow for greater flexibility.

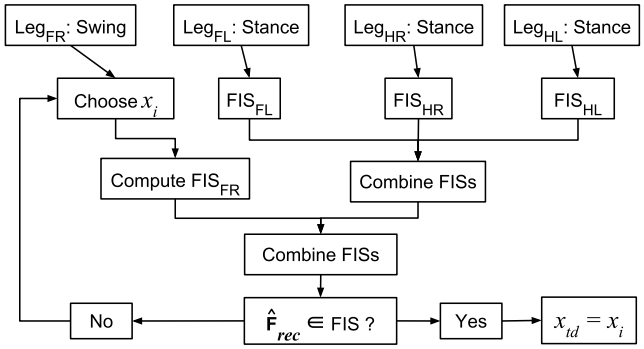

Fig. 3. Example of the push recovery algorithm applied to a quadruped in the case of 3 stance legs and one swing leg. The first step, not shown here, is the calculation of the remaining number of nodes before the next leg enters swing phase. This step allows the computation of the FIS as $\hat{\mathscr{F}}_{x_i \to x_f}$.

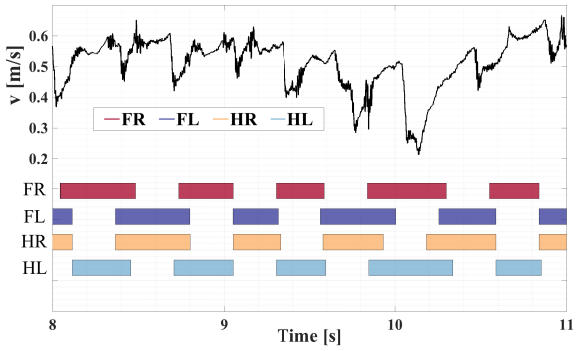

Fig. 4. Nontime-based gait emergence. Stance periods are not constrained to a fixed timing but rather they autonomously adapt. Data is presented from a hardware experiment with marginal utility threshold of 0.7. FR: front right, FL: front left, HR: hind right, HL: hind left.

in 3D. Briefly, control of the robot uses a PD law to regulate the body's height [35], and quadratic programming for instantaneous contact force distribution to manage balance (as in [35]). For push recovery, lateral foot placement is coordinated by a capture point heuristic, while in the sagittal plane it is coordinated by the FIS-based method detailed above. The reader is referred to [34] for further details on these control components. The nominal height of the hips above the ground was 0.5m, and nominal swing phase time was 250ms. Unless otherwise specified, the leg utility threshold was 15%, and the strategy for foot placement used 0.9 for the ratio of forward braking and propelling impulse capability (blue in Fig. 2). Two major takeaways can be seen from the experiments in this section and notably in Fig. 4. First is that the stance phase, and therefore the gait, is not time-constrained but rather adapts to the movement of the body. Second is that the legs move relatively independently of each other[6].

A. Hardware Results

Here we present results of experiments such as gait emergence during locomotion on a treadmill at different speeds, locomotion on a partially-moving walkway, and autonomously walking as a reaction to being pulled by someone. All experiments are shown in the supporting video.

[6]except for making sure the neighboring legs are in stance before entering a swing phase.

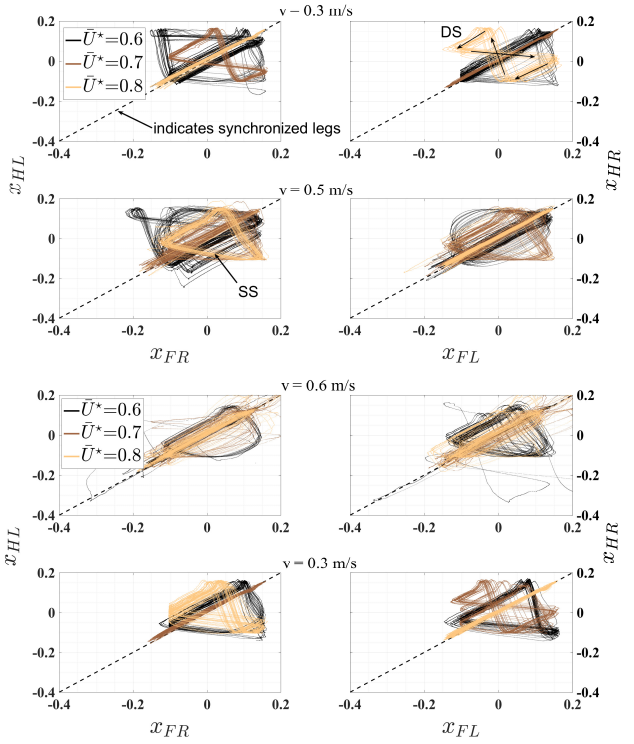

Fig. 5. Gait transitions with speed as a function of the marginal utility threshold. On the left are shown the phase portraits of the front right foot versus hind left foot positions for different speeds. On the right the same is shown for the other diagonal pair. More explanation is in the text. DS and SS denote double and single support for a diagonal pair, respectively.

1) Autonomous Gait Emergence and the Marginal Utility Threshold: The leg utility control framework presented here has successfully allowed for gait emergence and gait transitions with speed on the MIT Cheetah 3. The robot started from rest with symmetric foot positions. It was given a commanded forward velocity of 0.3m/s to 0.5m/s to 0.6m/s and back again to 0.3m/s. Experiments were repeated for different marginal utility (MU) thresholds $\bar{U}^\star$.

Figure 5 shows the position of the front right foot versus the hind left and similarly for the other diagonal pair. The effects of different speeds and different MU thresholds are shown. A figure-eight shape (as for $\bar{U}^\star = 0.7$ in the top left panel or for $\bar{U}^\star = 0.8$ in the top right panel of Fig. 5) indicates the presence of two double support and two single support periods for the diagonal pair of legs. A triangular shape indicates a double support, 2 single support, and potentially one short double flight phase. A line coinciding with the diagonal indicates synchronization of the diagonal pair of legs. With this insight, we observe the emergence of lateral sequence walk (L-walk, [36]) and 3-beat (that we coin "half-trot") gaits for lower speeds, and half-trot and trot gaits for higher speeds. Note that for $\bar{U}^\star = 0.6$, due to the symmetric starting position, the emerging gait tends to be a half-trot at the start, whereas it is a L-walk when decreasing the speed from 0.6 to 0.3m/s.

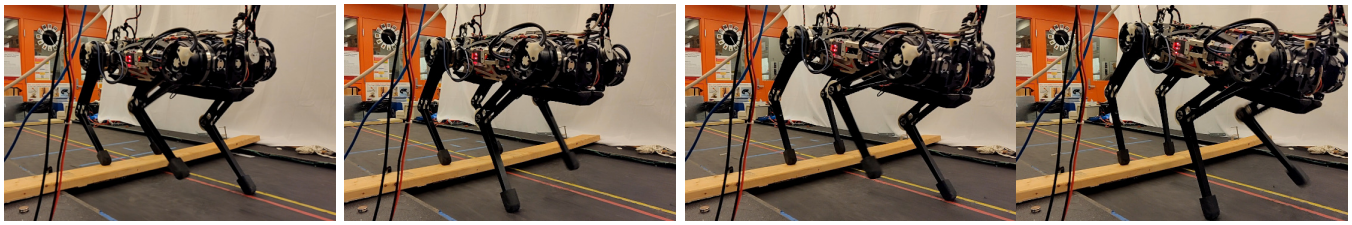

Fig. 6. Gait adaptation to a partially moving walkway. The speed of the treadmill closely matches that of the CoM. The leg utility control framework allows for instantaneous appropriate adaptation, whereby only the legs on the moving treadmill locomote.

Besides enabling gait emergence, the leg utility framework also allows the propensity for gait transitions to be tuned with a single parameter: the marginal utility threshold. Fig. 5 shows that a higher MU threshold favors 2- and 3-beat gaits (trot and half-trot), whereas lower MU thresholds favor 3- to 4-beat gaits (half-trot and walk). This could be explained by noting that a lower $\bar{U}^\star$ means the leg is able to enter swing phase only when the other legs have a sizable contribution to the overall FIS. This will tend to happen when there are 3 legs on the ground or 2 legs in the early part of their stance, and explains the occurrence of both 4-beat (walk) and 3-beat (half-trot) gaits. Note that while the nominal swing onset position (given by the utility threshold) is around -0.15m, the marginal utility threshold (second layer in Sec. III-B) can override this to delay swing onset beyond the nominal position when necessary (see Fig. 5). Finally, note that the pseudo-periodicity of trajectories may be indicative of non-optimality but also of adaptability and flexibility.

2) Stepping on a partially-moving walkway: A challenging and novel context for locomotion occurs when the legs experience different ground speeds. We test our framework in this context by having some legs step on a treadmill while the others step on an immobile board fixed above the moving surface. Because the leg utility framework reasons about the remaining impulse capabilities to flexibly generate gaits, the robot adapts instantly so that the legs on the immobile part do not cycle while the others do. This behavior happens whether one or two legs are placed on the immobile board.

3) Disturbance recovery: Another challenge considered was an experiment roughly equivalent to push recovery. The robot stood on an immobile treadmill, then the treadmill was turned on with a high speed that accelerated the system. The treadmill was then abruptly turned off, imparting an acceleration in the opposite direction. The robot used the algorithm shown in Fig. 3 to select recovery footsteps, without any input from a human operator. This inertia-based disturbance was successfully and autonomously counteracted by placing the feet back and forth in response to the negative and positive accelerations of the treadmill.

4) Taming the Cheetah: In this experiment an individual was walking and pulling the robot on a leash. In response, the robot kept walking, autonomously deciding on step positions and sequencing. We emphasize that the response was completely autonomous with no manual control.

B. Simulation Results

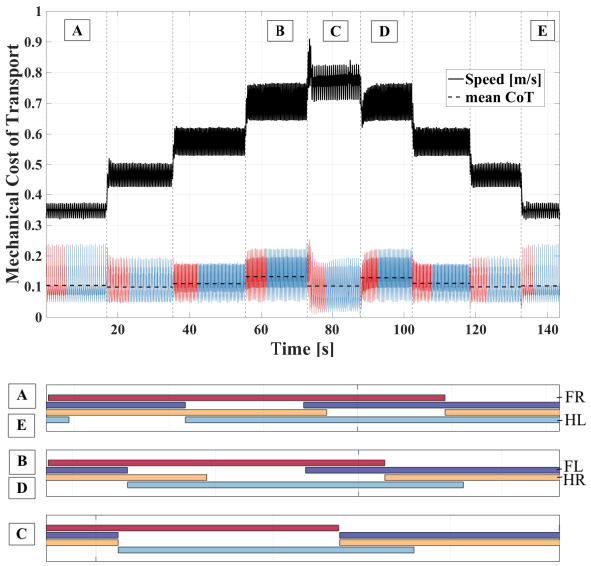

Fig. 7. Change of mechanical cost of transport with gait transitions and typical gaits in segments A-E. The typical gaits are taken after speed change and eventual gait transition, i.e. in the blue region of the corresponding segment in the top graph. Experiments were performed with $\bar{U}^\star = 0.63$.

This section shows 3D simulation results that further showcase properties of our framework. Dynamic simulation was performed using detailed models of Cheetah 3 from [37], with nonlinear spring-damper contact models as in [38]. Sensor noise and quantization effects were modelled according to manufacturer specifications, and a state estimator was used for state feedback [34].

1) Gait transitions and Cost of Transport: Interestingly, even though not explicitly programmed, gait transitions with speed are accompanied with abrupt cost of transport (CoT) changes. Fig. 7 shows a reduction of the mechanical CoT by 21-23% with gait transition (segment C compared to B and D in Fig. 7). Segments B and D exhibit a transitioning gait, neither a fully defined walk nor a fully defined trot. It is a 4-beat gait with 2 relatively short double flight phases (2 legs in the air at the same time). Segment C however exhibits a more defined 3-beat gait with 2 significant double flight phases. The transition to this gait brings the mechanical CoT to a level comparable to those of segments A and E, at low speed and exhibiting an L-walk gait.

2) Adaptation to injuries: The leg utility framework has also allowed accommodation of hardware problems such as a restricted range of motion. Fig. 8 shows such a case where

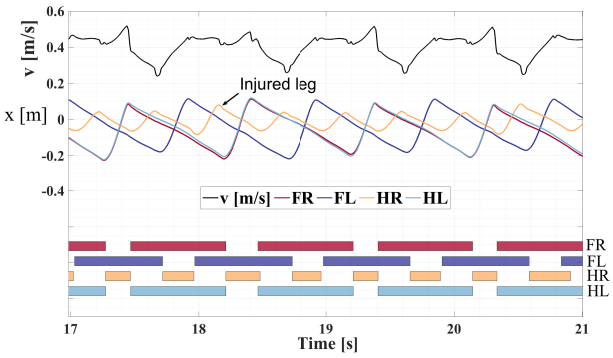

Fig. 8. Adaptation to injuries. The hind right (HR) leg represents a 'broken' leg with restricted range of motion.

the range of motion of the hind right (HR) leg was restricted around the resting position, mean walking speed was 0.4m/s and $\bar{U}^\star = 0.6$. It can be seen that successful gait adaptation was achieved, where the 'broken' leg makes short contacts while the other legs adapt accordingly.

V. Discussion

In this paper we presented a new control strategy that considers the impulse capabilities of the legs to know when and where to step, and which legs to use. Bringing to the front the inherent inseparability of motion from time, we proposed a new way of tackling locomotion from a high level. Computation of the feasible impulse set and associated leg utility metrics have allowed for nontime-based gait emergence and adaptation. Gaits that emerged in normal conditions were L-walk, half-trot and trot, on top of the adaptation to challenging situations. Indeed, the current framework has allowed to propose a Capture-Point-like recovery that is inherently applicable to multi-legged robots, providing both information on where to step as well as which leg to use for stepping. This feature is in contrast with the widely-successful Capture Point heuristic originally developed for a single leg [39].

In previous work, we presented results including push recovery, robust gait transitions [40] and walking over rough terrain [41]. The novelty of this paper however stems from the leg utility framework unifying low-level reflex-like mechanisms (such as take off) with high level decision-making (such as reasoning about foothold selection for push recovery). While previously footfall sequences and timings were predefined, the unification of touchdown and lift-off decision making through consideration of the FIS allowed for an integrated adaptive approach, thanks to which the robot transitions between *unprescribed* behaviors as fit to the situation. In particular, leg synchronization (as in trot or bounding [16]) is not enforced, thus allowing asynchronous leg movements. The practicality of this difference is seen in the experiments where the robot walks on a partially-moving walkway. Such experiments and results are unique to the framework we present in this paper.

The work herein borrows inspiration from recent advances that have used instantaneous wrench cones within planning and control [24]–[30], [35]. We have argued, however, that while wrench cones are suitable for instantaneous constraints, impulse considerations will be more suitable for higher level abstraction and reasoning about locomotion overall, since impulses take into account the dynamics over extended time frames. While there is information lost in this compression of time, the results show that the FIS enables unified treatment of multi-legged stepping in a variety of novel contexts.

The work is also related to recent advances by Winkler et al. [21]. Their work leaves footfall timings flexible during a centralized motion planning process that optimizes a gait for a fully-specified environment. By contrast, our paper provides online autonomous gait emergence and disturbance recovery, resulting in stable and robust locomotion without the need for precise prior knowledge of the terrain. Naturally, the combined benefits of their approach and ours may offer benefits longer term. In the future, we also expect our approach to work well in other environments (such as stairs) by making appropriate coordinate transformations.

As for CPGs, while they can offer a convenient dynamical systems framework, they are inherently periodic. In contrast, operating in the real world imposes constant deviation from periodicity. Additional layered strategies often complement CPGs to produce discrete actions and disturbance recovery. In contrast, our physics-based framework is general enough to provide both periodicity and aperiodicity where needed.

This said, an important assumption of this work is the ability to estimate the trajectory of the CoM, for example by assuming a constant speed within a stride. In the future, we plan to iterate between optimizing CoM trajectories with [16] and selecting footholds with the control method presented here. While the current framework can be used as is for 3D touchdown and swing onset position decision-making from a theoretical standpoint, a major hurdle is the ensuing computational cost. To handle this challenge, we envision 3D extensions of the FIS methodology by treating the fore/aft and lateral impulses in a decoupled way ($2\times$2D) and combining their outputs. This approach would be computationally viable. It is currently unclear whether the benefits of coupled 3D FIS computations would outweigh their costs, and this question will be investigated in future work. We also acknowledge that our framework may not provide the optimal gait for any given speed. In particular, a speed-dependent parameter change for touchdown and swing onset may be desired to improve interlimb coordination. We also remark that we do not use preview models to assess rotational stability, which is enforced through the swing leg policy and the QP balance control. While the swing policy in its current form is not suitable for such gaits as pacing or bounding, we expect the extension with an "angular momentum impulse set" to provide better insights into the dynamics and thus allow for greater flexibility in the gaits that emerge.

Finally, in contrast with most of the work in the literature, the robot is not constrained to a predefined gait that operates even when locomotion is not needed. As leg movement occurs only when needed, this has implications on energy consumption, making our control strategy more energy efficient, as well as better aligned with our expectations for how an animal might reasonably operate in a similar situation.

VI. Conclusion

We emphasized a new outlook on locomotion that reasons about the coordination of leg impulses over time. The novel notions of FIS and leg utility metrics provided a unified physics-based framework for adaptive lift-off and touchdown for gait emergence and adaptation. The concept of impulse generation further provides a new scientific hypothesis for biological gait control, e.g., as a determinant of CPGs' genesis. Future work includes investigating 3D computations, and integrating the framework with a PR-MPC one.

ACKNOWLEDGMENT

The first author thanks A. Wang for insightful discussions, and Q. Nguyen and B. Katz for help in the experiments.

References

[1] S. Aoi, P. Manoonpong, Y. Ambe, F. Matsuno, and F. Wörgötter, "Adaptive control strategies for interlimb coordination in legged robots: A review," *Frontiers in Neurorobotics*, vol. 11, p. 39, 8 2017.

[2] D. F. Hoyt and C. R. Taylor, "Gait and the energetics of locomotion in horses," *Nature*, vol. 292, no. 5820, pp. 239–240, 1981.

[3] A. Ruina, J. E. Bertram, and M. Srinivasan, "A collisional model of the energetic cost of support work qualitatively explains leg sequencing in walking and galloping, pseudo-elastic leg behavior in running and the walk-to-run transition," *Journal of Theoretical Biology*, vol. 237, no. 2, pp. 170–192, 2005.

[4] A. Hreljac, "Determinants of the gait transition speed during human locomotion: Kinematic factors," *Journal of Biomechanics*, vol. 28, no. 6, pp. 669–677, 1995.

[5] C. T. Farley and C. R. Taylor, "A mechanical trigger for the trot-gallop transition in horses," *Science*, vol. 253, no. 5017, pp. 306–308, 1991.

[6] K. Wampler and Z. Popovic, "Optimal gait and form for animal locomotion," *ACM Transactions on Graphics*, vol. 28, no. 3, 2009.

[7] P. Ramdya, R. Thandiackal, R. Cherney, T. Asselborn, R. Benton, A. J. Ijspeert, and D. Floreano, "Climbing favours the tripod gait over alternative faster insect gaits," *Nature Communications*, vol. 8, p. 14494, 2017.

[8] V. Barasuol, J. Buchli, C. Semini, M. Frigerio, E. R. De Pieri, and D. G. Caldwell, "A reactive controller framework for quadrupedal locomotion on challenging terrain." in *ICRA*, 2013, pp. 2554–2561.

[9] A. J. Ijspeert, "Central pattern generators for locomotion control in animals and robots: a review," *Neural networks*, vol. 21, no. 4, pp. 642–653, 2008.

[10] D. Owaki and A. Ishiguro, "A quadruped robot exhibiting spontaneous gait transitions from walking to trotting to galloping," *Scientific Reports*, vol. 7, no. 1, p. 277, 2017.

[11] H. Kimura, Y. Fukuoka, and A. H. Cohen, "Biologically inspired adaptive walking of a quadruped robot," *Philosophical Trans. of the Royal Society of London A*, vol. 365, no. 1850, pp. 153–170, 2007.

[12] Y. Fukuoka, Y. Habu, and T. Fukui, "Analysis of the gait generation principle by a simulated quadruped model with a CPG incorporating vestibular modulation," *Biological Cybernetics*, vol. 107, no. 6, pp. 695–710, 2013.

[13] ——, "A simple rule for quadrupedal gait generation determined by leg loading feedback: a modeling study," *Scientific Reports*, vol. 5, p. 8169, 2015.

[14] D. J. Hyun, S. Seok, J. Lee, and S. Kim, "High speed trot-running: Implementation of a hierarchical controller using proprioceptive impedance control on the MIT Cheetah," *The International Journal of Robotics Research*, vol. 33, no. 11, pp. 1417–1445, 2014.

[15] H.-W. Park, P. M. Wensing, and S. Kim, "High-speed bounding with the MIT Cheetah 2: Control design and experiments," *Int. Journal of Robotics Research*, vol. 36, no. 2, pp. 167–192, 2017.

[16] G. Bledt, P. M. Wensing, and S. Kim, "Policy-regularized model predictive control to stabilize diverse quadrupedal gaits for the MIT cheetah," in *IEEE/RSJ Int. Conf. on Intelligent Robots and Systems*, 2017, pp. 4102–4109.

[17] J. D. Carlo, P. M. Wensing, B. Katz, G. Bledt, and S. Kim, "Dynamic locomotion in the MIT Cheetah 3 through convex model-predictive control," in *IEEE/RSJ Int. Conf. on Intelligent Robotics and Systems*, 2018.

[18] C. D. Bellicoso, F. Jenelten, C. Gehring, and M. Hutter, "Dynamic locomotion through online nonlinear motion optimization for quadrupedal robots," *IEEE Robotics and Automation Letters*, vol. 3, no. 3, pp. 2261–2268, July 2018.

[19] H.-W. Park, P. M. Wensing, and S. Kim, "Online planning for autonomous running jumps over obstacles in high-speed quadrupeds," in *Robotics: Science and Systems Conf.*, 2015, pp. 1–9.

[20] A. Herdt, H. Diedam, P.-B. Wieber, D. Dimitrov, K. Mombaur, and M. Diehl, "Online walking motion generation with automatic footstep placement," *Advanced Robotics*, vol. 24, no. 5-6, pp. 719–737, 2010.

[21] A. W. Winkler, C. D. Bellicoso, M. Hutter, and J. Buchli, "Gait and trajectory optimization for legged systems through phase-based end-effector parameterization," *IEEE Robotics and Automation Letters*, vol. 3, no. 3, pp. 1560–1567, 2018.

[22] A. K. Valenzuela, "Mixed-integer convex optimization for planning aggressive motions of legged robots over rough terrain," Ph.D. dissertation, Massachusetts Institute of Technology, 2016.

[23] T. Marcucci, R. Deits, M. Gabiccini, A. Bicchi, and R. Tedrake, "Approximate hybrid model predictive control for multi-contact push recovery in complex environments," in *IEEE-RAS Int. Conf. on Humanoid Robotics*, Nov 2017, pp. 31–38.

[24] T. Bretl and S. Lall, "Testing static equilibrium for legged robots," *IEEE Transactions on Robotics*, vol. 24, no. 4, pp. 794–807, 2008.

[25] S. Caron, Q.-C. Pham, and Y. Nakamura, "Leveraging cone double description for multi-contact stability of humanoids with applications to statics and dynamics." in *Robotics: Science and Systems*, 2015.

[26] H. Audren and A. Kheddar, "3-d robust stability polyhedron in multi-contact," *IEEE Transactions on Robotics*, 2018.

[27] S. Caron and A. Kheddar, "Multi-contact walking pattern generation based on model preview control of 3D COM accelerations," in *IEEE-RAS Int. Conf. on Humanoid Robots*, 2016, pp. 550–557.

[28] Z. Qiu, A. Escande, A. Micaelli, and T. Robert, "Human motions analysis and simulation based on a general criterion of stability," in *International Symposium on Digital Human Modeling*, 2011, pp. 1–8.

[29] R. Orsolino, M. Focchi, C. Mastalli, H. Dai, D. G. Caldwell, and C. Semini, "Application of wrench-based feasibility analysis to the online trajectory optimization of legged robots," *IEEE Robotics and Automation Letters*, vol. 3, no. 4, pp. 3363–3370, Oct 2018.

[30] V. Samy, S. Caron, K. Bouyarmane, and A. Kheddar, "Post-impact adaptive compliance for humanoid falls using predictive control of a reduced model," in *IEEE-RAS Int. Conf. on Humanoid Robotics*, 2017, pp. 655–660.

[31] S. Hirai, "Analysis and planning of manipulation using the theory of polyhedral convex cones," Ph.D. dissertation, 1991.

[32] D. Avis, "A revised implementation of the reverse search vertex enumeration algorithm," in *DMV SEMINAR*, vol. 29. Springer, 2000, pp. 177–198.

[33] S. Barthélemy and P. Bidaud, "Stability measure of postural dynamic equilibrium based on residual radius," *Advances in Robot Kinematics: Analysis and Design*, pp. 399–407, 2008.

[34] G. Bledt, M. J. Powell, B. Katz, J. D. Carlo, P. M. Wensing, and S. Kim, "MIT Cheetah 3: Design and control of a robust, dynamic quadruped robot," in *IEEE/RSJ Int. Conf. on Intelligent Robotics and Systems*, 2018.

[35] M. Focchi, A. d. Prete, I. Havoutis, R. Featherstone, D. G. Caldwell, and C. Semini, "High-slope terrain locomotion for torque-controlled quadruped robots," *Autonomous Robots*, vol. 41, pp. 259–272, 2016.

[36] M. Hildebrand, "Symmetrical gaits of horses," *Science*, vol. 150, no. 3697, pp. 701–708, 1965.

[37] P. M. Wensing, S. Kim, and J. E. Slotine, "Linear matrix inequalities for physically consistent inertial parameter identification: A statistical perspective on the mass distribution," *IEEE Robotics and Automation Letters*, vol. 3, no. 1, pp. 60–67, Jan 2018.

[38] M. Azad and R. Featherstone, "A new nonlinear model of contact normal force," *IEEE Transactions on Robotics*, vol. 30, no. 3, pp. 736–739, June 2014.

[39] J. Pratt, J. Carff, S. Drakunov, and A. Goswami, "Capture point: A step toward humanoid push recovery," in *IEEE-RAS Int. Conf. on Humanoid Robots*, 2006, pp. 200–207.

[40] D. J. Hyun, J. Lee, S. Park, and S. Kim, "Implementation of trot-to-gallop transition and subsequent gallop on the MIT Cheetah I," *Int. Journal of Robotics Research*, vol. 35, no. 13, pp. 1627–1650, 2016.

[41] G. Bledt, P. M. Wensing, S. Ingersoll, and S. Kim, "Contact model fusion for event-based locomotion in unstructured terrains," in *IEEE Int. Conf. on Robotics and Automation*, 2018.